Title	Wave pictures of three coupled waves on electron beams and slow wave circuits
Sub Title	
Author	藤田, 広一(Fujita, Hiroichi) 藤岡, 知夫(Fujioka, Tomoo)
Publisher	慶応義塾大学藤原記念工学部
Publication year	1966
Jtitle	Proceedings of the Fujihara Memorial Faculty of Engineering Keio University (慶応義塾大学藤原記念工学部研究報告). Vol.19, No.74 (1966.) ,p.121(11)- 138(28)
JaLC DOI	
Abstract	The dispersion equation for three coupled waves is analysed by numerical method and ω-β diagrams are given. They show occasionally very different features from two waves case, details of which are discussed in this paper, and some examples of application are proposed.
Notes	
Genre	Departmental Bulletin Paper
URL	https://koara.lib.keio.ac.jp/xoonips/modules/xoonips/detail.php?koara_id=KO50001004-00190074-0011

Wave Pictures of Three Coupled Waves on Electron Beams and Slow Wave Circuits

(Received May 25, 1966)

Hiroichi FUJITA*

Tomoo FUJIOKA**

Abstract

The dispersion equation for three coupled waves is analysed by numerical method and $\omega-\beta$ diagrams are given. They show occasionally very different features from two waves case, details of which are discussed in this paper, and some examples of application are proposed.

I. Introduction

The amplification mechanism of traveling-wave type tubes, such as traveling wave tubes and double-stream amplifiers among many micro wave tubes, are illustrated by the so-called coupled mode theory[1)-4)]. Two kinds of longitudinal space charge waves, fast wave and slow wave, exist in a one-dimentional electron beam, the former carrying positive power and the latter carrying negative power[5),6)]. The amplification phenomenon of the traveling-wave tube can be understood by the mutual interaction resulting in the distributed coupling between the electromagnetic wave on slow wave circuit and the slow wave in an electron beam, while the double-stream amplifier depends on the mutual interaction between the fast wave on one of the two beams and the slow wave on the other beam. Thus, the active coupling, the coupling between a wave carrying negative power and the other one carrying positive power, makes growing wave, while passive coupling, coupling

* 藤田広一, Associate Professor, Faculty of Engineering, Keio University.

** 藤岡知夫, Instructor, Faculty of Engineering, Keio University.

1) J. R. Pierce; "Traveling Wave Tube", van Nostrand, (1950).

2) J. R Pierce; "Coupling of Modes of Propagation", Jour. Appl. Phys., vol. 25, p. 179, (Feb. 1954).

3) J. R. Pierce; "The Wave Pictures of Microwave Tubes", B.S.T.J., vol. 33, p. 1343, (Nov. 1954).

4) M. C. Pease; "Generalized Coupled Mode Theory", Jour. Appl. Phys. vol. 32, p. 1736, (Sep. 1961).

5) W. C. Hahn; "Small Signal Theory of Velocity-Modulated Electron Beams", G.E. Rev., vol. 42, p. 258, (June 1939).

6) S. Ramo; "Space Charge and Field Waves in an Electron Beam", Phys. Rev., vol. 56, p. 276, (Aug. 1939).

between two waves both carrying power of the same sign, produces two propagating waves.

In the latter case, power is transferred from one wave to the other in a half beat wave cycle. The phenomenon called Kompfner dip is understood by this concept. These coupling phenomena between two waves are easily understood by "$\omega-\beta$ diagram". Fig. 1 is the case of active coupling, and it shows that propagation constants, β's, afthr coupling become a set of conjugate complex numbers in the neighbourhood of a point (ω_0, β_0), which is the intersectional point of β_1 and β_2, the propagation constants of two waves prior to coupling. Fig. 2 is the case of passive coupling and shows two propagating waves, of which phase constants differ slightly ih the neighbourhood of a point (ω_0, β_0).

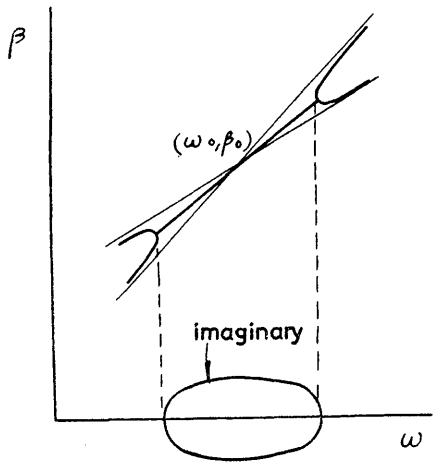

Fig. 1. The signs of blow power of two waves are opposite.

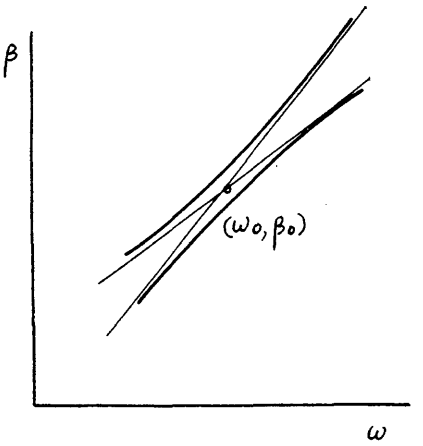

Fig. 2. The signs of blow power of two waves are same.

In this way the distributed interaction phenomenon between two waves is understood. However, what will happen when more waves than two make distributed interaction simultaneously. If we confine the problem within traveling wave tube, Pierce has treated it in his earlier work[1]. Solymar has treated a case in which there is no interaction between a set of three waves, which is the same for travelling wave tube, and considered the region in which growing wave exists[7].

The general dispersion equations for n coupled waves has already been given[8], which determins eigen values of β's.

In this paper the authors will analyse by numerical method the case of coupling

7) L. Solymar; "Some Properties of Three Coupled Waves", IRE, MTT-8, p. 284, (May 1960).

8) N. Saito; "Electro Magnetic Circuit Theory of Electron Beams", Ohmu sha, (1960).

among three waves, of which β cross at a point on the $\omega-\beta$ diagram prior to coupling, and discuss the singular properties of wave pictures.

II. Analysis and calculation

The following assumptions underlie the analysis:

(1) Waves are represented by one-dimentional electromagnetic equations.

(2) Wave amplitude is so small that small signal theory can be applied.

(3) When wave propagates, there is no loss on transmission lines. It is supposed that the straight-lines on the $\omega-\beta$ diagram give approximate values for the behavior of three waves and they meet at one point (ω_0, β_0), as Fig. 3. Straight-lines give good approximations for any waves in a small region. These straight-lines can be described by the following equations:

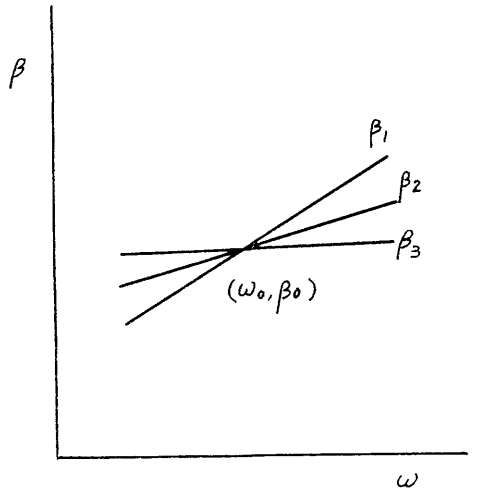

Fig. 3. The waves prior to coupling.

$$\left.\begin{aligned}\beta_1-\beta_0&=a(\omega-\omega_0)\,,\\ \beta_2-\beta_0&=b(\omega-\omega_0)\,,\\ \beta_3-\beta_0&=c(\omega-\omega_0)\,.\end{aligned}\right\} \tag{1}$$

Here a, b and c are the gradients.

To calculate the distributed interaction between three waves, we consider a new coordinate system, whose origin is (ω_0, β_0) and weose abscissa is β_3. That is,

$$\left.\begin{aligned}&\beta_1'=\beta_1-\beta_3=a'\omega'\,,\\ &\beta_2'=\beta_2-\beta_3=b'\omega'\,,\\ &a'=a-c,\ b'=b-c,\ \omega'=\omega-\omega_0\,.\end{aligned}\right\} \tag{2}$$

We can write the equations of the distributed interaction between three waves as follows:

$$\left.\begin{aligned}\frac{dE_1}{dz}&=-j\beta_1E_1+C_{12}E_2+C_{13}E_3\ ,\\ \frac{dE_2}{dz}&=C_{21}E_1-j\beta_2E_2+C_{23}E_3\ ,\\ \frac{dE_3}{dz}&=C_{31}E_1+C_{32}E_2-j\beta_3E_3\ .\end{aligned}\right\}\tag{3}$$

Here E_1, E_2 and E_3 are the amplitudes of three waves and C_{ik} is the coupling factor per unit length from k wave to i wave, satisfying the condition

$$C_{ik}=\mp C_{ki}^*\ .\tag{4}$$

where * is a symbol denoting conjugate number, and (−) indicates the case when both i and k waves carry the powers of the same sign, while (+) indicates when they carry the powers of opposite sign. Thus, when wave 3 is taken as a standard, it is enough for us to calculate only four cases as indicated in Table 1.

Table 1. Combination of the sign of flow power. S and 0 indicate the direction of flow power is same as and opposite to wave 3, respectively.

Wave \ Case	I	II	III	IV
Wave 1	S	S	0	0
Wave 2	S	0	0	S

When E_1, E_2 and E_3 are written in the form

$$E_1=A_1e^{-\Gamma z},\quad E_2=A_2e^{-\Gamma z},\quad E_3=A_3e^{-\Gamma z}\ .$$

and substituted into (3), we find the following dispersion equation determining the eigen values of Γ,

$$\begin{vmatrix}\Gamma-j\beta_1 & C_{12} & C_{13}\\ C_{21} & \Gamma-j\beta_2 & C_{23}\\ C_{31} & C_{32} & \Gamma-j\beta_3\end{vmatrix}=0\ .\tag{5}$$

We express C_{ik} as follows,

$$C_{12}=|C_{12}|e^{j\theta_{12}},\quad C_{23}=|C_{23}|e^{j\theta_{23}},\quad C_{31}=|C_{31}|e^{j\theta_{31}}\tag{6}$$

$$\varphi=\theta_{12}+\theta_{23}+\theta_{31}\ .\tag{7}$$

For lossless transmission line, values for θ_1, θ_2 and θ_3 are given in Table 2. Then from (7) and Table 2, we have

Table 2. Value of θ_{ik}.

The sign of flow power		θ_{ik}
i	k	
+	+	$\frac{\pi}{2}$
−	−	$-\frac{\pi}{2}$
+	−	$\frac{\pi}{2}$
−	+	$-\frac{\pi}{2}$

$$\omega=\pm\frac{\pi}{2}\,. \tag{8}$$

As (2), we rewrite Γ as follows:

$$\Gamma=j(\gamma+\beta_3)\,. \tag{9}$$

Now, from (2), (6) and (7), (5) reduces to the following:

$$\gamma^3-(a'\omega'+b'\omega')\gamma^2+\{(a'\omega')(b'\omega')\mp|C_{12}|^2\mp|C_{23}|^2\mp|C_{31}|^2\}\gamma\pm a'\omega'|C_{23}|^2\pm b'\omega'|C_{31}|^2 \\ -2|C_{12}|\,|C_{23}|\,|C_{31}|\sin\varphi=0\,. \tag{10}$$

Where upper sign indidates the case when the power of k and i waves are of the same signs, and lower sign when they are of the opposite signs. According to (8), we have

$$\sin\varphi=\pm1\,.$$

If we substitute $-\gamma$ and $-\omega'$ for γ and ω' respectively into the result obtained by the calculation of equation (10) for $\sin\varphi=-1$, we can obtain also the result for $\sin\varphi=1$. The calculation of one of the two cases is enough, so we now consider the case $\sin\varphi=-1$.

To calculate the equation (10), we normalize it by the greatest value, $|C_{ik}|_{est}$, among $|C_{ik}|$'s.

$$\frac{a'\omega'}{|C_{ik}|_{est}}=x,\quad \frac{\gamma}{|C_{ik}|_{est}}=y,\quad \frac{b'}{a'}=k,\quad \frac{|C_{i'k'}|}{|C_{ik}|_{est}}=\alpha_1,\ \alpha_2\,. \tag{11}$$

$$0\leq k\leq1,\quad 0\leq\alpha_1,\ \alpha_2\leq1\,.$$

In virtue of (11) we may also write (10) as

$$y^3-(k+1)xy^2+\{kx^2\mp\alpha_1^2\mp\alpha_2^2\mp1\}y+Ax+2=0\,. \tag{12}$$

$|C_{12}|$ is maximum: $\alpha_1=\frac{|C_{23}|}{|C_{12}|}$, $\alpha_2=\frac{|C_{31}|}{|C_{12}|}$, $A=\pm\alpha_1^2\pm k\alpha_2^2$. (13)

$$|C_{23}| \text{ is maximum:} \quad \alpha_1=\frac{|C_{12}|}{|C_{23}|}, \quad \alpha_2=\frac{|C_{31}|}{|C_{23}|}, \quad A=\pm 1\pm k\alpha_2^2 . \tag{14}$$

$$|C_{31}| \text{ is maximum:} \quad \alpha_1=\frac{|C_{12}|}{|C_{31}|}, \quad \alpha_2=\frac{|C_{23}|}{|C_{31}|}, \quad A=\pm\alpha_2^2\pm k . \tag{15}$$

III. Results and discussions

Case I.

This is the case when the transmission powers of three waves are all of the same sign. In this case, if it is assumed that $\alpha_1=\alpha_2=1$, namely, all the coupling factors are equal, (is) is written as

$$y^3-(k+1)xy^2+(kx^2-3)y+(k+1)x+2=0 . \tag{16}$$

Two examples of calculation results of (16) are shown in Figs. 4 and 5. From the results of calculations, the following conclusions are obtained:

i) Since there exists no wave which transmits power of opposite sign, γ's are never complex numbers. Accordingly, three propagating waves occur in general, and three waves after coupiing are written as

$$\left.\begin{aligned} E_1(z)&=e^{j\beta_3 z}\sum_1^3 A_{1n}e^{j\gamma_n z} ,\\ E_2(z)&=e^{j\beta_3 z}\sum_1^3 A_{2n}e^{j\gamma_n z} ,\\ E_3(z)&=e^{j\beta_3 z}\sum_1^3 A_{3n}e^{j\gamma_n z} ,\\ \gamma_n&=y_n|C_{ik}|_{est} . \end{aligned}\right\} \tag{17}$$

Where $y_{n's}$ are the roots of (16) and real numbers, and A_{mn}'s are in general constants of complex numbers which are determined by (3) and initial conditions.

ii) For $k\to 0$, one of roots of y becomes unity for any value of x. This can be shown as follows: When $k\to 0$ in (16), $(y-1)\{y^2-(x-1)y-(x+2)\}=0$. Thus, y becomes unity.

For $k\to 1$, one of roots of y becomes $(x+1)$ on the diagram. This can be shown also as follows: When $k\to 1$ in (16), we obtain $\{y-(x+1)\}\{y^2-(x-1)y-2\}=0$.

iii) When both α_1 and α_2 are not unity, the results are essentially the same and the same wave pictures are obtained.

Case II.

This is the case when the power of wave 1 and wave 3 are of the same sign, and wave 2 of the opposite sign. In this case, the following equations to be solved are obtained from (12) to (15).

$$|C_{12}| \text{ is max.:} \quad y^3-(1+k)xy^2+(kx^2+\alpha_1^2-\alpha_2^2+1)y+(k\alpha_2^2-\alpha_1^2)x+2\alpha_1\alpha_2=0 . \tag{18}$$

$$|C_{23}| \text{ is max.:} \quad y^3-(1+k)xy^2+(kx^2+\alpha_1^2-\alpha_2^2+1)y+(k\alpha_2^2-1)x+2\alpha_1\alpha_2=0 . \tag{19}$$

$|C_{31}|$ is max.: $y^3-(1+k)xy^2+(kx^2+\alpha_1^2+\alpha_2^2-1)y+(k-\alpha_2^2)x+2\alpha_1\alpha_2=0$. (20)

Examples calculation results are shown in Figs. 6 to 19. From the results, the following conclusions are obtained:

i) In general there is a set of conjugate complex number roots of y in the neighbourhood of $x=0$. Accordingly a growing wave occurs in the coupled waves. In this case three waves after coupling can be written as

$$\left.\begin{aligned} &E_n(z)=e^{j\beta_3 z}\sum_{m=1}^{3}A_{nm}e^{j\gamma_m z}\ . \\ &\gamma_m=y_m|C_{ik}|_{est}\ ,\quad y_m=(y_m)_{\text{real}}+j(y_m)_{\text{jmaginary}}\ . \end{aligned}\right\} \tag{21}$$

where y_m's are the roots of (12) and A_{mn}'s are determined by (13) and initial conditions, as in Case I.

The Growing wave is not always an increasing wave and it can be an evanescent wave[9),10)]. But we are not interested here in distinguishing the growing waves.

ii) As indicated in Fig. 6 and 7, the region where x gives complex roots to y spreads to $-\infty$ as $k\to 0$. The limit of $k=0$ seems to correspond to the result obtained by Pierce for the case where space charge parameter QC of traveling-wave tube equals zero[1)]. Also as seen in Figs. 6 and 8, the region spreads to $+\infty$ as $k\to 1$. Mathematically, for the case $\alpha_1=\alpha_2=1$ this can be shown as follows; If we substitute $\alpha_1=\alpha_2=1$ into (18), (19) and (20), we obtain

$$y^3-(1+k)xy^2+(kx^2+1)y-(1-k)x+2=0\ . \tag{22}$$

And if we substitute $y=0$ into (22), we obtain $x=\dfrac{2}{1-k}$, which we again substitute into (22), obtaining $y\left(y-\dfrac{1+k}{1-k}\right)^2=0$. At the point where the imaginary part of the root becomes zero, (22) has equal roots. Accordingly, it is ascertained that, for $x<\dfrac{2}{1-k}$, y has complex root. On the other hand, if we substitute $(1-k)$ for k and put $y=0$ into (20), we get $x=\dfrac{2}{k}$. And when we substitue $x=-\dfrac{2}{k}$ into (20), we get $\left(y+\dfrac{2}{k}\right)(y+1)^2=0$. Thus the above obtained results yield a region where the growing wave takes place, $-\dfrac{2}{k}<x<\dfrac{2}{1-k}$.

When α_1, $\alpha_2\neq 0$, we will get the same results as obtained in the preceding calculation. But it is difficult to get mathematically the exact region where complex root occurs. So we anticipate the region from obtained diagrams. For example, the region when $|C_{31}|$ is maximum is

9) P. A. Sturrock; "Kinematics of Growing Waves", Phy. Rev., vol. 112, p. 1488, (Dec. 1958).

10) Y. Sawayama; "Studies on Growihg Waves", Report of Microwave Tube Committees, I.E.C.E. of Japan, (Jan. 1962).

$$-\frac{2}{k}\frac{|C_{23}|}{|C_{31}|}<x<\frac{2}{1-k}\frac{|C_{12}|}{|C_{31}|}\,.$$

iii) There is only a little change in the wave picture when α_1 and α_2 are not equal to unity nor zero. Figs. 9 and 10 show the examples when $k=0.5$.

iv) When $|C_{12}|=0$, the wave picture shows a singular form. That is, the imaginary part of y changes according to the relation between $|C_{31}|$ and $|C_{23}|$, i.e., when $|C_{31}|=|C_{23}|$, the imaginary part is separated into two parts, which are tangent to each other at the origin, as indcitated in Fig. 11; when $|C_{31}|<|C_{23}|$, the two parts blend and imaginary part shows an ordinary pattern as indicated in Fig. 12; when $|C_{31}|>|C_{23}|$, y has no complex root and there are three propagating waves, as indicated in Fig. 13.

Mathematically, these matters are shown as follows: when $|C_{23}|>|C_{31}|$, we substitute $\alpha_1=0$ and $x=0$ into (17) and get $y^3+(1+\alpha_2^2)y=0$.
Accordingly, for $x=0$, y has two imaginary roots. when $|C_{23}|<|C_{31}|$, we substitute $\alpha_1=1$ and $x=0$ in (18) and get $y^3-(1-\alpha_2^2)y=0$.
Since $1-\alpha_2^2>0$, y has three real roots and no imaginary term occures.

v) The result for $|C_{23}|=0$ equals the above (iv), i.e., when $|C_{12}|=|C_{31}|$, the imaginary part is separated into two parts at the origin; when $|C_{12}|>|C_{31}|$, two parts blend and shows ordinary pattern; when $|C_{12}|<|C_{31}|$, there is no imaginary part. (Figs. 14, 15, 16)

vi) Wave pictures for $|C_{31}|=0$ differ entirely from those of iv) and v). y has always complex roots in the neighbourhood of the origin. (Figs. 17, 18 and 19)

For $k\to1$ or $k\to0$, the region for imaginary part spreads. (Fig. 19)

Case III.

This is the case when the power of wave 1 and wave 2 are of the same sign and wave 3 is of the opposite sign. In this case, the equations to be solved are as follows:

$|C_{12}|$ is max.: $y^3-(1+k)xy^2+(kx^2+\alpha_1^2+\alpha_2^2-1)y-(\alpha_1^2+k\alpha_2^2)x+2\alpha_1\alpha_2=0$. (23)

$|C_{23}|$ is max.: $y^3-(1+k)xy^2+(kx^2-\alpha_1^2+\alpha_2^2+1)y-(k\alpha_2^2+1)x+2\alpha_1\alpha_2=0$. (24)

$|C_{31}|$ is max.: $y^3-(1+k)xy^2+(kx^2-\alpha_1^2+\alpha_2^2+1)y-(k+\alpha_2^2)x+2\alpha_1\alpha_2=0$. (25)

i) In general, in the region of the neighbourhood of $x=0$, y has a set of conjugate complex roots and a growing wave occurs in the coupling wave. In this case, each wave after coupling is written as (21), as in Case II. The different point of wave picture, however, from Case II is that the curve of imaginary part is separated into two parts, as in Figs. 20 and 25.

ii) For $k\to1$, the region where y has complex root spreads to $x=\pm\infty$. For $k\to1$, the region becomes narrower. Figs. 20, 21, and 22 show the examples for $\alpha_1=\alpha_2=1$. Mathematically, this is shown as follows: if we substitute $\alpha_1=\alpha_2=1$ into (23), we

obtain

$$y^3-(1+k)xy^2+(kx^2+1)y-(1+k)x+2=0\,. \tag{26}$$

When we substitute $x=2$ into (26), we get $(y-2k)(y-1)^2=0$. Now, it has been shown that the imaginary part becomes zero at $x=2$, and y has equal roots. Since we can see from figures that another root of y is given by the value of x when $y=x$, the point where the imaginary part is zero is obtained by substituting $y=x$ into (26), resulting in $x=\frac{2}{k}$, which we substitute again into (26) and obtain $\left(y-\frac{2}{k}\right)(y-1)^2=0$. Accordingly, the region where y has complex root is written as $2<x<\frac{2}{k}$.

Let us find the value of x where the imaginary part becomes zero for $x<0$. It is difficult to find this value exactly, but it may be said that this value is greater than $-\left(2+\frac{2}{k}\right)$. This is shown as follows; we substitute $x=-\left(2+\frac{2}{k}\right)$ into (26), we obtain $(y-1)\left(y^2+\frac{2k^2+3k+2}{k}y+\frac{2k^2+6k+2}{k}\right)=0$. It can be easily verified that this equation has three real roots for $0\leqq k\leqq 1$. Accordingly the region is $-\left(2+\frac{2}{k}\right)<x<2$. If we substitute $k\to 0$ in these two inequalities, the region of x spreads to $\pm\infty$. For $k\to 1$, the region becomes narrower.

iii) The imaginary part changes according to the sign of $|C_{12}|-|C_{23}|$, i.e., when $|C_{12}|=|C_{23}|$, two imaginary parts occur, which are tangent to each other, as indicated in Figs. 20 to 23; when $|C_{12}|>|C_{23}|$, two parts are separated, as in Fig. 24; when $|C_{12}|<|C_{23}|$, two parts blend, as in Figs. 25 and 26.

iv) For $|C_{12}|=0$, one imaginary part occurs in the neighbourhood of $x=0$, as in Fig. 26.

v) For $|C_{23}|=0$, wave picture is similar to iii); when $|C_{12}|=|C_{31}|$, the two imaginary parts occur, which are tangent to each other, as in Fig. 27; when $|C_{12}|>|C_{31}|$, two parts are separated into two independent parts, as in Fig. 28; when $|C_{12}|<|C_{32}|$, two parts blend to become one part.

vi) For $|C_{23}|=0$, the wave picture is the same as in iv). The imaginary parts, which are tangent to each other when $|C_{12}|=|C_{23}|$, are separated into two independent parts when $|C_{12}|>|C_{23}|$, and inversely blend to one part again when $|C_{12}|<|C_{23}|$, as indicated in Figs. 30 to 32.

Case IV

This is the case when the powers of wave 2 and wave 3 are of the same sign and the power of wave 1 is of the opposite sign. In this case, the equations to be solved are, from (12) to (15), as follows:

$$|C_{12}| \text{ is max.:}\quad y^3-(1+k)xy^2+(kx^2+\alpha_1^2+\alpha_2^2-1)y+(\alpha_1^2-k\alpha_2^2)x+2\alpha_1\alpha_2=0\,. \tag{27}$$

$|C_{23}|$ is max.: $y^3-(1+k)xy^2+(kx^2+\alpha_1^2+\alpha_2^2-1)y+(1-k\alpha_2^2)x+2\alpha_1\alpha_2=0$. (28)

$|C_{31}|$ is max.: $y^3-(1+k)xy^2+(kx^2+\alpha_1^2-\alpha_2^2+1)y+(k-\alpha_2^2)x+2\alpha_1\alpha_2=0$. (29)

Now we substitute $(y+x)$ for y, $(1-k)$ for k and $(-x)$ for x in (23), (24) and (25), we obtain (27), (28) and (29). Thus we can find entirely the wave pictures of Case IV from the results of Case III. The characteristics in the following are the same as in Case III.

i) The imaginary parts of y consist, in general, of two parts,

ii) When $\alpha_1=\alpha_2=1$, the region where complex roots appear is, from the same discussion in Case III,

$$-\frac{2}{1-k}<x<-2 \quad \text{and} \quad -2<x<2+\frac{2}{1-k}\ .$$

Thus, for $k\to 1$, the region spreads and for $k\to 0$, the region becomes narrower. This results can be applied also when $\alpha_1\fallingdotseq 1$ and $\alpha_2\fallingdotseq 1$.

iii) When $|C_{12}|\leqq|C_{23}|$, two imaginary parts occur and when $|C_{12}|>|C_{23}|$, they blend.

iv) For $|C_{12}|=0$, the imaginary part is separated when $|C_{23}|\geqq|C_{31}|$ and blends when $|C_{23}|<|C_{31}|$.

v) For $|C_{31}|=0$, we have similar wave pictures as in iv), i.e., the imaginary part is separated when $|C_{12}|<|C_{23}|$, and blends when $|C_{12}|>|C_{23}|$.

vi) When $|C_{23}|=0$, the imaginary part consists of one part and shows the ordinary type.

IV. Some Examples of application

I. Application for coupled helices[11]

Calculation in this paper is partly intended in preparations for some experiments, that the authors are planning, to measure noise parameter in electron beam by using coupled helices. The results in this paper give useful information for using coupled helices.

II. Super wide-band traveling wave tube

Since the region of x where y has complex conjugate roots spreads to $x=\pm\infty$ when $k\to 0$ or $k\to 1$ in Case II, the possibility of traveling wave tube with super wide-band range of frequency tuning is suggested. This will be realized by coupling of slow wave circuit with double electron streams. However, the effect of space-charge wave harmonics and the wide-band matching at the ends of the slow wave circuit will be the problems.

III. Active filter with two pass bands.

There exist two frequency tuning regions, which yield growing waves, in such

11) J. S. Cook, R. Kompfner and C. F. Quate; "Coupled Helices", B.S.T.J., vol. 35, p. 127, (Jan. 1956).

wave pictures as Figs. 28 and 31. Accordingly, it is possible to use this effect as active filter with two pass bands. This can be realized by double structure helices, one of which couples with the slow-wave of an electron beam.

Acknowledgements

The authors wish to thank K. Tsuda and K. Ohmori for their numerical calculations and assistances in this research.

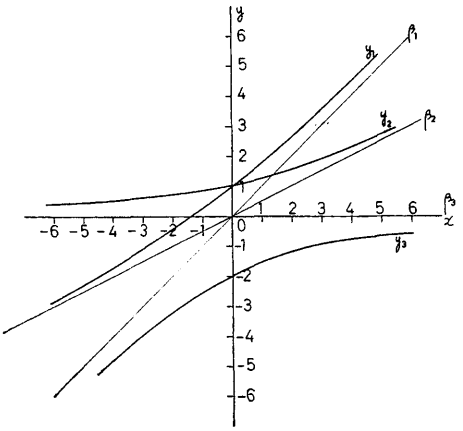

Fig. 4. Case I.
The signs of flow power of three waves are all same.

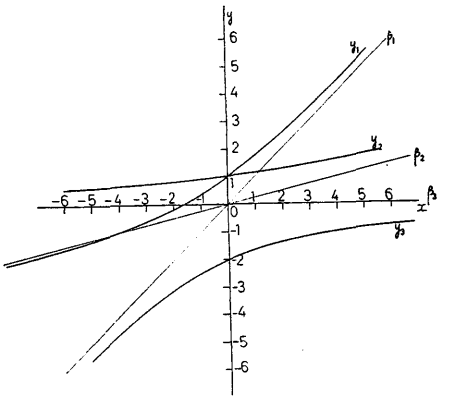

Fig. 5. Case I.
The signs of flow power of three waves are all same.

$$k=\frac{1}{4},\quad \alpha_1=\alpha_2=1.$$

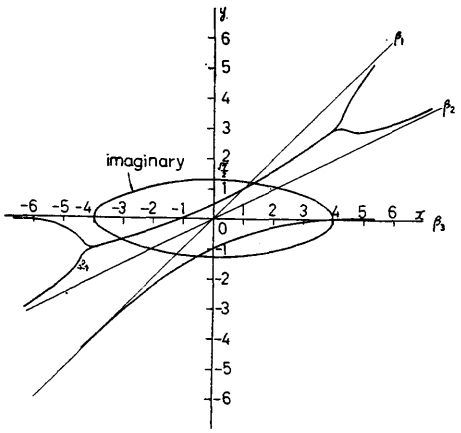

Fig. 6. Case II.
The sign of wave 2 is opposite to the oters.

$$k=0.5,\quad |C_{12}|=|C_{23}|=|C_{31}|.$$

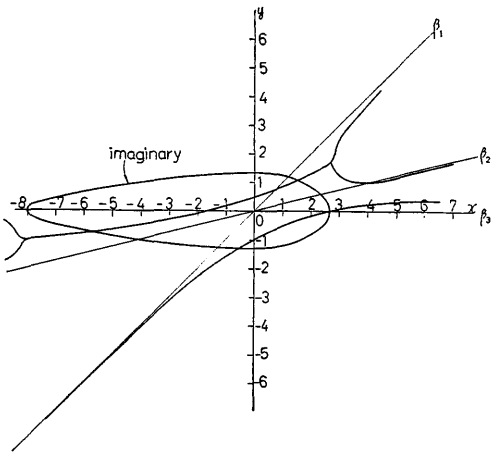

Fig. 7. Case II.
The sign of flow power of wave 2 is opposite to the others.

$$k=\frac{1}{4},\quad |C_{12}|=|C_{23}|=|C_{31}|.$$

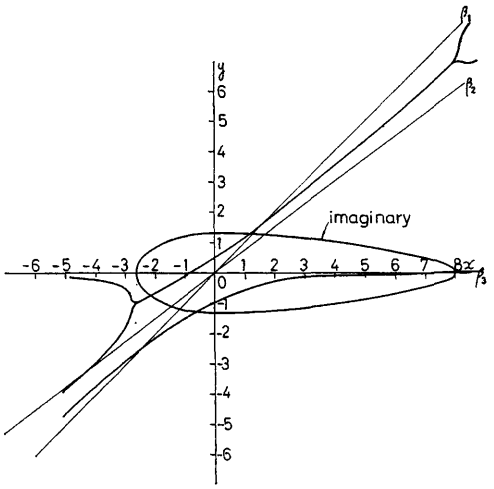

Fig. 8. Case II.
The sign of flow power of wave 2 is opposite to the others.
$k=\frac{3}{4}$, $|C_{12}|=|C_{23}|=|C_{31}|$.

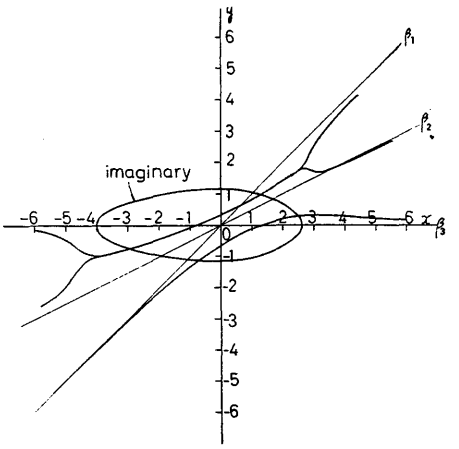

Fig. 9. Case II.
The sign of flow power of wave 2 is opposite to the others.
$k=\frac{1}{2}$, $|C_{12}|=|C_{31}|=\frac{1}{\sqrt{2}}|C_{23}|$.

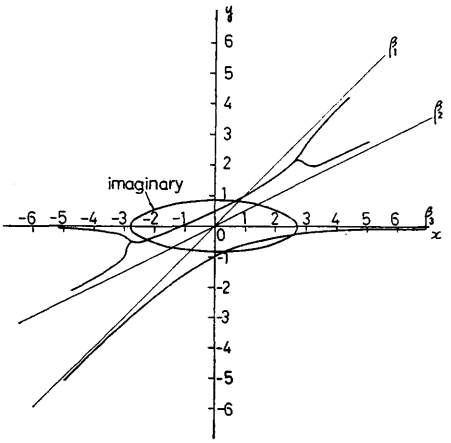

Fig. 10. Case II.
The sign of flow power of wave 2 is opposite to the others.
$k=\frac{1}{2}$, $|C_{12}|=|C_{23}|=\frac{1}{\sqrt{2}}|C_{31}|$.

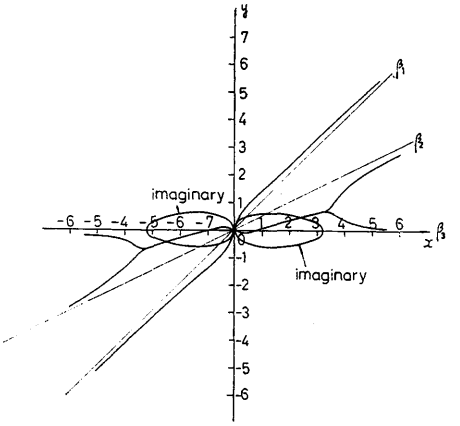

Fig. 11. Case II.
The sign of flow power of wave 2 is opposite to the others.
$k=\frac{1}{2}$, $|C_{12}|=0$, $|C_{31}|=|C_{23}|$.

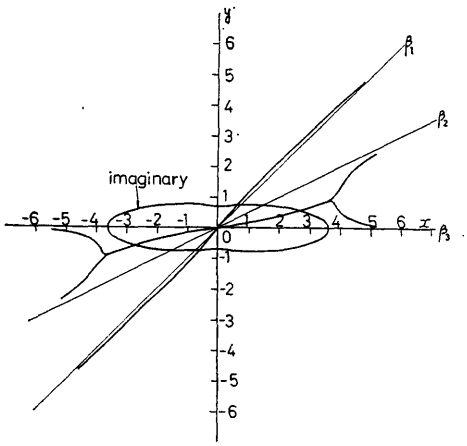

Fig. 12. Case II.
The sign of flow power of wave 2 is opposite to the others.
$k=\frac{1}{2}$, $|C_{12}|=0$, $|C_{23}|=\sqrt{2}|C_{31}|$.

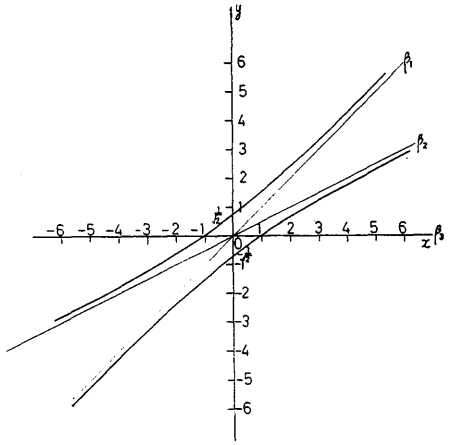

Fig. 13. Case II.
The sign of flow power of wave 2 is opposite to the others.
$k=\frac{1}{2}$, $|C_{12}|=0$, $|C_{23}|=\frac{1}{\sqrt{2}}|C_{31}|$.

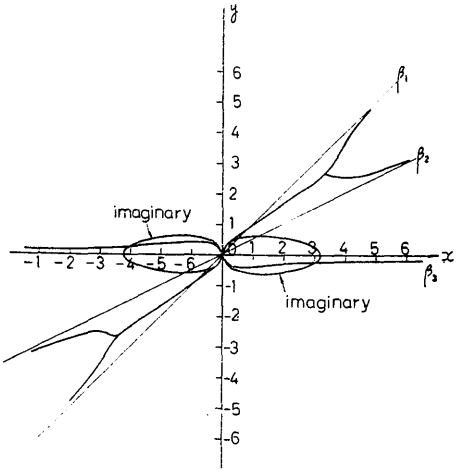

Fig. 14. Case II.
The sign of flow power of wave 2 is opposite to the others.
$k=\frac{1}{2}$, $|C_{23}|=0$, $|C_{12}|=|C_{31}|$.

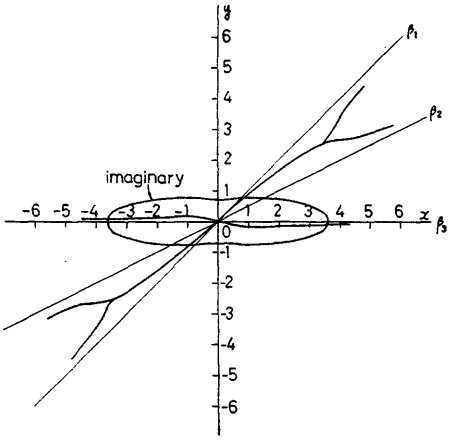

Fig. 15. Case II.
The sign of flow power of wave 2 is opposite to the others.
$k=\frac{1}{2}$, $|C_{23}|=0$, $|C_{12}|=\sqrt{2}|C_{31}|$.

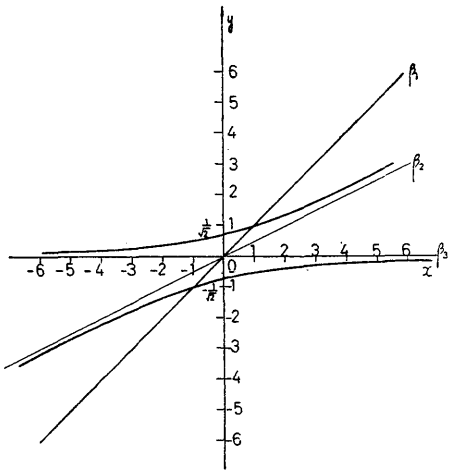

Fig. 16. Case II.
The sign of flow power of wave 2 is opposite to the others.
$k=\frac{1}{2}$, $|C_{23}|=0$, $|C_{12}|=\frac{1}{\sqrt{2}}|C_{31}|$.

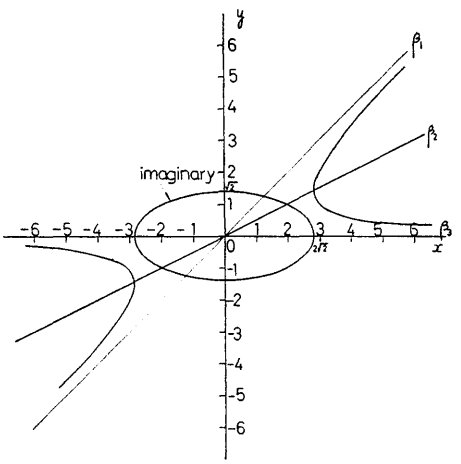

Fig. 17. Case II.
The sign of flow power of wave 2 is opposite to the others.
$k=\frac{1}{2}$, $|C_{31}|=0$, $|C_{12}|=|C_{23}|$.

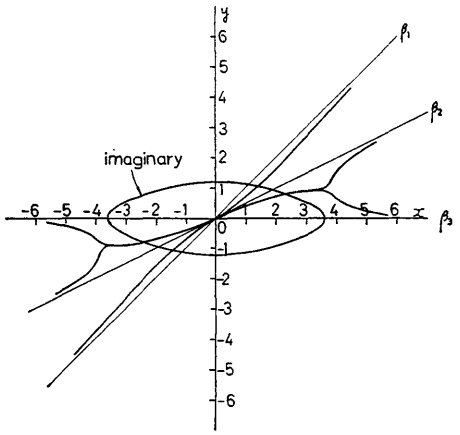

Fig. 18. Case II.
The sign of flow power of wave 2 is opposite to the others.
$k=\frac{1}{2}$, $|C_{31}|=0$, $|C_{23}|=\sqrt{2}|C_{31}|$.

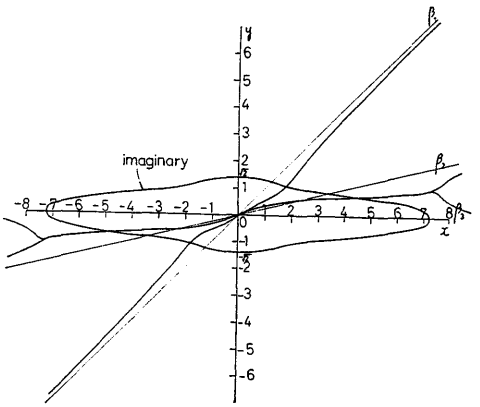

Fig. 19. Case II.
The sign of flow power of wave 2 is opposite to the others.
$k=\frac{1}{4}$, $|C_{31}|=0$, $|C_{12}|=|C_{23}|$.

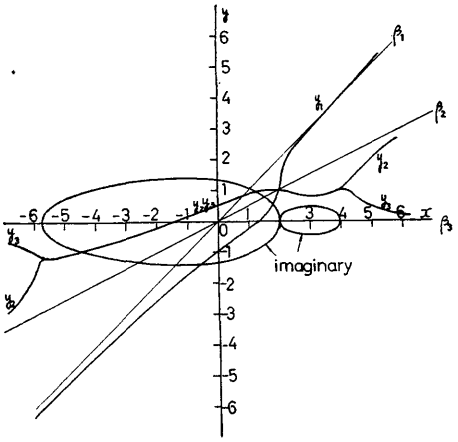

Fig. 20. Case II.
The sign of flow power of wave 3 is opposite to the others.

$k=\frac{1}{2}$, $|C_{12}|=|C_{23}|=|C_{31}|$.

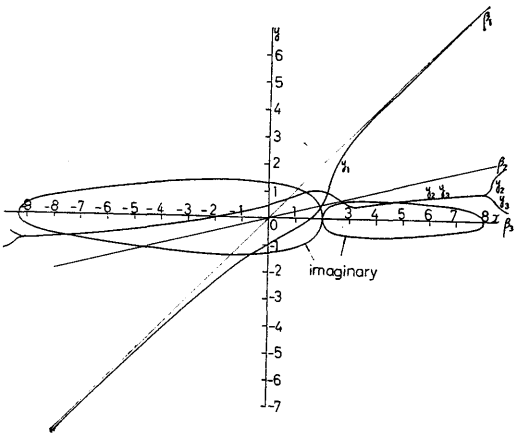

Fig. 21. Case III.
The sign of flow power of wave 3 is opposite to the others.

$k=\frac{1}{4}$, $|C_{12}|=|C_{23}|=|C_{31}|$.

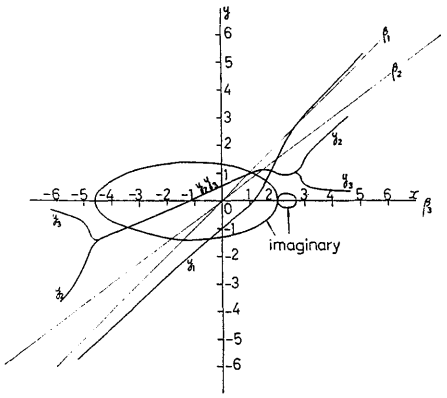

Fig. 22. Case III.
The sign of flow power of wave 3 is opposite to the others.

$k=\frac{3}{4}$, $|C_{12}|=|C_{23}|=|C_{31}|$.

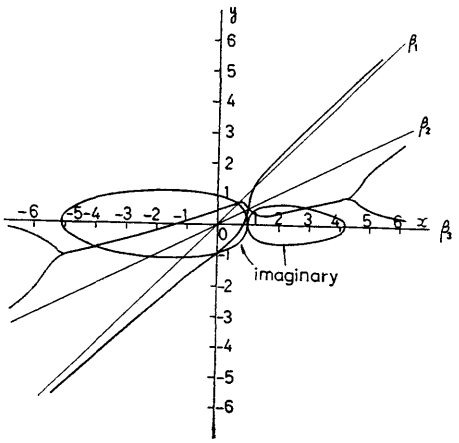

Fig. 23. Case III.
The sign of flow power of wave 3 is opposite to the others.

$k=\frac{1}{2}$, $|C_{12}|=|C_{23}|=\sqrt{2}\,|C_{31}|$.

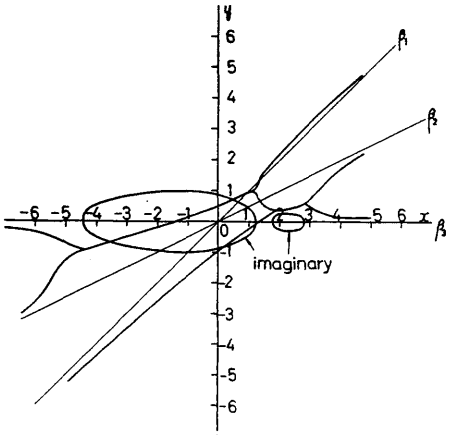

Fig. 24. Case III.
The sign of flow power of wave 3 is opposite to the others.

$$k=\frac{1}{2},\ |C_{23}|=|C_{31}|=\frac{1}{\sqrt{2}}|C_{12}|.$$

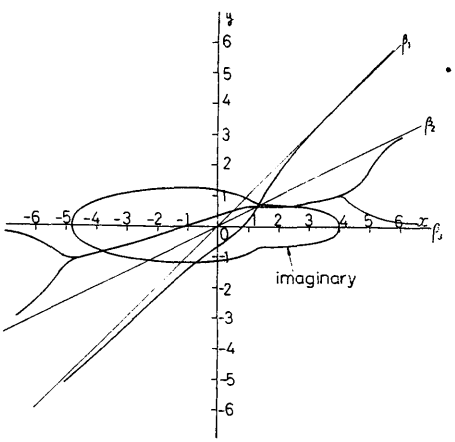

Fig. 25. Case III.
The sign of flow power of wave 3 is opposite to the others.

$$k=\frac{1}{2},\ |C_{12}|=|C_{31}|=\frac{1}{\sqrt{2}}|C_{23}|.$$

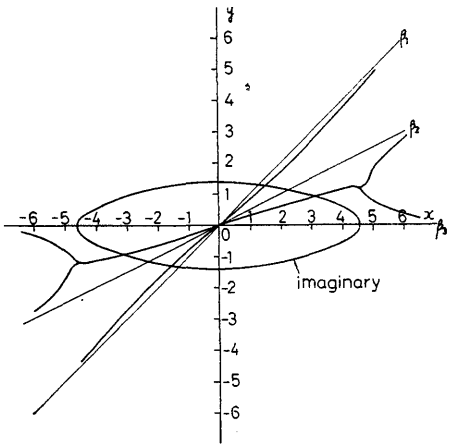

Fig. 26. Case III.
The sign of flow power of wave 3 is opposite to the others.

$$k=\frac{1}{2},\ |C_{12}|=0,\ |C_{23}|=|C_{31}|.$$

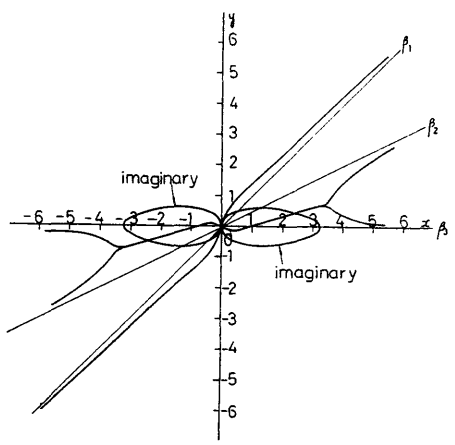

Fig. 27. Case III.
The sign of flow power of wave 3 is opposite to the others.

$$k=\frac{1}{2},\ |C_{23}|=0,\ |C_{12}|=|C_{31}|.$$

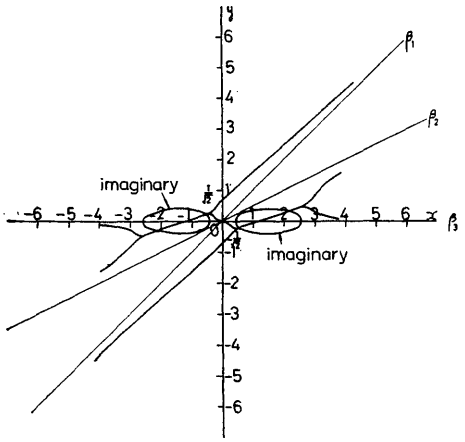

Fig. 28. Case III.
The sign of flow power of wave 3 is opposite to the others.
$k=\frac{1}{2}$, $|C_{23}|=0$, $|C_{12}|=\sqrt{2}\,|c_{31}|$.

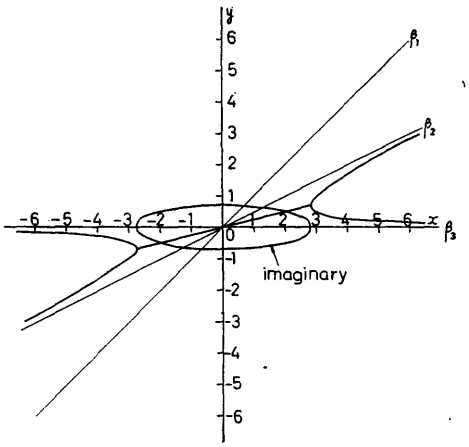

Fig. 29. Case III.
The sign of flow power of wave 3 is opposite to the others.
$k=\frac{1}{2}$, $|C_{23}|=0$, $|C_{12}|=\frac{1}{\sqrt{2}}|C_{31}|$.

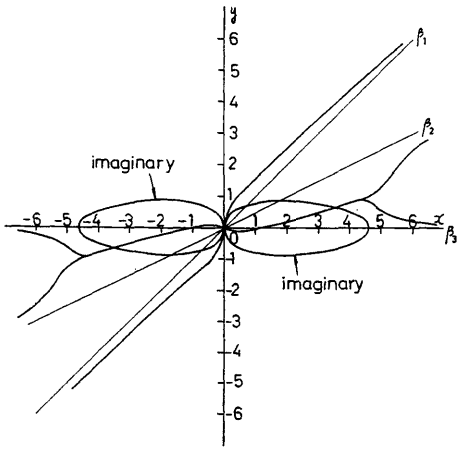

Fig. 30. Case III.
The sign of flow power of wave 3 is opposite to the others.
$k=\frac{1}{2}$, $|C_{31}|=0$, $|C_{12}|=|C_{23}|$.

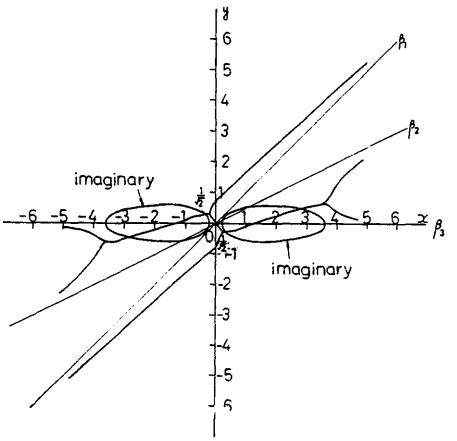

Fig. 31. Case III.
The sign of flow power of wave 3 is opposite to the others.
$k=\frac{1}{2}$, $|C_{31}|=0$, $|C_{12}|=\sqrt{2}\,|C_{23}|$.

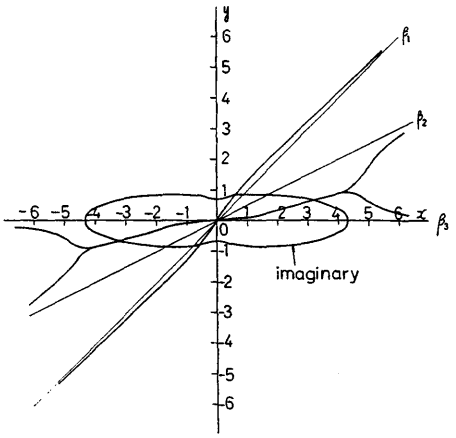

Fig. 32. Case III.
The sign of flow power of wave 3 is opposite to the others.

$$k=\frac{1}{2},\quad |C_{31}|=0,\quad |C_{12}|=\frac{1}{\sqrt{2}}|C_{23}|.$$